Published in final edited form as:
Eur J Neurosci. 2008 October ; 28(7): 1301–1315. doi:10.1111/j.1460-9568.2008.06437.x.

Temporally structured replay of neural activity in a model of entorhinal cortex, hippocampus and postsubiculum

Michael E. Hasselmo
Center for Memory and Brain, Department of Psychology and Program in Neuroscience, Boston University, 2 Cummington St., Boston, Massachusetts 02215, (617) 353-1397, FAX: (617) 358-3296, hasselmo@bu.edu.

Abstract

The spiking activity of hippocampal neurons during REM sleep exhibits temporally structured replay of spiking occurring during previously experienced trajectories (Louie and Wilson, 2001). Here, temporally structured replay of place cell activity during REM sleep is modeled in a large-scale network simulation of grid cells, place cells and head direction cells. During simulated waking behavior, the movement of the simulated rat drives activity of a population of head direction cells that updates the activity of a population of entorhinal grid cells. The population of grid cells drives the activity of place cells coding individual locations. Associations between location and movement direction are encoded by modification of excitatory synaptic connections from place cells to speed modulated head direction cells. During simulated REM sleep, the population of place cells coding an experienced location activates the head direction cells coding the associated movement direction. Spiking of head direction cells then causes frequency shifts within the population of entorhinal grid cells to update a phase representation of location. Spiking grid cells then activate new place cells that drive new head direction activity. In contrast to models that perform temporally compressed sequence retrieval similar to sharp wave activity, this model can simulate data on temporally structured replay of hippocampal place cell activity during REM sleep at time scales similar to those observed during waking. These mechanisms could be important for episodic memory of trajectories.

Keywords

episodic memory; grid cells; head direction cells; memory retrieval; postsubiculum; rat

INTRODUCTION

Neurophysiological data from the hippocampus demonstrates that spiking activity of place cells during rapid eye movement (REM) sleep shows temporally structured replay of sequences that occurred during prior waking behavior (Louie and Wilson, 2001). This replay occurs at time scales similar to those during waking (Louie and Wilson, 2001). Recordings during REM periods of 60 to 240 secs duration (mean 114 secs) showed temporal scaling factors ranging from 0.55 to 2.49 (mean 1.4). A scaling factor of 1.0 means replay occurs at the same speed as waking, and a scaling factor of 1.4 means a 60 sec period of REM matches a 43 sec period of waking. Other studies also show neural replay of previously experienced trajectories during waking (Foster and Wilson, 2006; Diba and Buzsaki, 2007; Johnson and Redish, 2007) and slow wave sleep (Skaggs and McNaughton, 1996; Lee and Wilson, 2002), but non-REM replay involves retrieval at a very compressed time scale.

Previous models have simulated the replay of sequences at a compressed time scale (Jensen and Lisman, 1996a, b; Levy, 1996; Tsodyks et al., 1996; Wallenstein and Hasselmo, 1997; Hasselmo and Eichenbaum, 2005). Fast replay occurs because associations are formed directly

between place cells representing sensory state, and the time window of modification of synapses during encoding is longer than the time scale of synaptic transmission during retrieval. In contrast, the model presented here forms associations between place cells coding sensory state and head direction cells coding the action leading to the next state. Persistent spiking in head direction cells allows updating of a continuous representation of space provided by modelled grid cells. The combination of persistent firing and a continuous representation of space allows simulation of the slower temporally structured replay observed during REM sleep.

Beyond the REM data (Louie and Wilson, 2001), this model was motivated by neurophysiological data showing: 1.) grid cell firing patterns in entorhinal cortex (Hafting et al., 2005; Sargolini et al., 2006; Fyhn et al., 2007), 2.) membrane potential oscillations in entorhinal cortex layer II (Alonso and Llinas, 1989; Dickson et al., 2000; Giocomo et al., 2007), 3.) persistent firing in deep entorhinal cortex neurons (Egorov et al., 2002; Fransén et al., 2006) and postsubiculum (Yoshida and Hasselmo, 2008), 4.) place cells in hippocampus (O'Keefe, 1976; O'Keefe and Burgess, 2005; McNaughton et al., 2006), and 5.) head direction cells in the postsubiculum (Taube et al., 1990b; Sharp et al., 2001; Taube and Bassett, 2003) and deep layers of entorhinal cortex (Sargolini et al., 2006). Data on differences in membrane potential oscillation frequency along the dorsal to ventral axis of entorhinal cortex (Giocomo et al., 2007) support the model of grid cells used here, in which grid cell oscillation phase integrates head direction input to code continuous space (Burgess et al., 2007; Hasselmo et al., 2007). Graded persistent firing occurs in deep entorhinal neurons during cholinergic modulation (Egorov et al., 2002), consistent with acetylcholine levels observed during waking and REM sleep (Marrosu et al., 1995). Persistent firing could allow deep entorhinal or postsubicular head direction cells to hold activity scaled to the speed and direction of retrieved movement to update the phase of grid cell oscillations. These cellular mechanisms allow an explicit representation of the time duration of sequences during retrieval, providing the temporally structured replay seen during REM sleep (Louie and Wilson, 2001). These simulations generate predictions about replay of grid cell and head direction cell activity during REM sleep.

METHODS

The temporally structured replay of place cell activity during REM sleep was simulated in a network model summarized in Figure 1. This model includes a population of grid cells based on data from recordings in the medial entorhinal cortex (Hafting et al., 2005;Sargolini et al., 2006;Fyhn et al., 2007). Grid cells were generated using a recent model of potential mechanisms for grid cell formation (Burgess et al., 2007;Giocomo et al., 2007;Hasselmo et al., 2007), as shown in Figure 2 for open field activity and Figure 3 for a circular track. The model also includes a population of place cells with place fields resembling data from recordings on linear tracks (Louie and Wilson, 2001;Lee et al., 2004a;Lee et al., 2004b). Place cells were generated using input from grid cells in a manner similar to other models (Fuhs and Touretzky, 2006;McNaughton et al., 2006;Rolls et al., 2006;Solstad et al., 2006;Franzius et al., 2007b;Molter and Yamaguchi, 2007). Place cell activity in the network is shown in Figure 4. Finally, the model includes a population of head direction cells based on neural activity recorded in deep layers of the entorhinal cortex (Sargolini et al., 2006) or postsubiculum (dorsal presubiculum) (Taube et al., 1990a;Taube and Burton, 1995;Sharp, 1996;Taube et al., 1996;Sharp et al., 2001;Taube and Bassett, 2003), as shown in Figure 5. The simulation of behavior will be described first, followed by description of the simulation of activity in different populations of neurons, followed by description of the mechanisms of encoding during waking due to synaptic modification, and finally the mechanism of retrieval during REM sleep.

Behavior on circular track

The temporally structured replay of place cell spiking activity during REM sleep was demonstrated in an experiment using a circular running track (Louie and Wilson, 2001). Therefore, the simulations presented here focus on the virtual rat running a circular trajectory during waking (encoding). This was simulated by starting a virtual rat running south at a fixed rate, and then modulating the velocity vector of running so that the rat would run around a circle with a diameter of 95 centimeters, matching the experimental apparatus. Unless otherwise noted, the virtual rat ran at a mean speed of 50 cm/sec for 24 seconds, resulting in a total arc length of 1200 cm, or about 4 cycles of the approximately 300 cm circumference of the circular track, but effects of variation in speed were also tested. After simulation of running in the circular track, the simulation was shifted to the REM sleep mode with no external input, and temporally structured replay was tested by reactivation of the pattern of grid cell, place cell and head direction cell activity from the first step of waking.

Grid cell model

Consistent with experimental data, the population of grid cells in the model includes neurons that fire with different size and spacing between firing fields, as well as different spatial phases relative to the environment. Orientation was kept consistent within a simulation, based on similarity of orientation within each local region of entorhinal cortex. These properties are obtained with the Burgess, Barry and O'Keefe model of grid cells (Burgess et al., 2005; O'Keefe and Burgess, 2005; Burgess et al., 2007). In this model, membrane potential oscillations in individual neurons interfere in a manner resulting in grid cell firing patterns. The difference in size and spacing of grid fields results from differences in the baseline frequency of membrane potential oscillations, consistent with experimental data showing differences in intrinsic membrane potential oscillation frequency along the dorsal to ventral axis of the medial entorhinal cortex (Giocomo et al., 2007; Hasselmo et al., 2007).

Data shows that the frequency of membrane potential oscillations is increased from baseline by depolarizing input (Alonso and Llinas, 1989; Alonso and Klink, 1993; Dickson et al., 2000; Giocomo et al., 2007). Thus, depolarizing input to superficial layers of entorhinal cortex (Caballero-Bleda and Witter, 1993) from head direction cells in the postsubiculum (Taube et al., 1990b; Sharp et al., 2001; Taube and Bassett, 2003) and deep layers of entorhinal cortex (Sargolini et al., 2006) could provide changes in oscillation frequency dependent upon head direction activity. In the Burgess model, speed-modulated head direction input alters oscillation frequency in different dendrites of entorhinal stellate cells in proportion to the speed of movement in different directions (Burgess et al., 2007; Giocomo et al., 2007; Hasselmo et al., 2007). The pattern of grid cell firing $g(t)$ arises due to interference of different frequencies induced by the integration of different head direction inputs. The model used in previous papers is described here by the following equation:

$$g_{jk}(t)=\Theta[\prod_{i}\{\cos(2\pi f_j t)+\cos((2\pi f_j(t+B\int_0^t \vec{h}_i(\tau)d\tau)+\vec{\varphi}_{jk})\}] \quad (1)$$

In this equation, $g_{jk}(t)$ represents the firing over time of a single grid cell with baseline frequency f_j and the dendritic oscillation phase vector $\vec{\varphi}_{ik}$. Π_i represents the product of the different dendritic oscillations receiving input from different components of the head direction vector with index i. Θ represents a Heaviside step function output (the model has output 1 for values above a threshold of 0.3, and output of zero otherwise). The intrinsic membrane potential oscillations have baseline frequency f_j for different populations of grid cells j. The frequencies of dendritic oscillations are modulated by input from a population of head direction cells with

activity represented by the vector $\vec{h}_i(t)$. This representation of head direction is described below and is mathematically equivalent to the Burgess model. This input is scaled by a constant B set to 0.00385 based on experimental data (Giocomo et al., 2007). The dendritic branches of a single grid cell have initial phases represented by the initial phase vector $\vec{\varphi}_{ik}$ that has an element for each component of input h_i and differs across individual grid cells k.

This model creates grid cell firing fields with spacing dependent upon modulation of the intrinsic oscillation frequency f_j (Giocomo et al., 2007; Hasselmo et al., 2007). The sum of the somatic oscillation with frequency f and each dendritic oscillation with frequency $f + fB\vec{h}(t)$ results in an interference pattern that has an envelope with a frequency equal to the difference of the two frequencies $fB\vec{h}(t)$. Note that this model can also generate grid cell patterns with direct interactions of dendritic oscillations in the absence of somatic oscillations (Hasselmo et al., 2007). Recent simulations show that dendritic oscillations tend to synchronize, but the same model presented here can be implemented by using neurons that show intrinsic persistent spiking at a stable frequency and can shift their phase transiently in response to depolarizing input (Hasselmo, 2008; Hasselmo and Brandon, 2008). This is consistent with extensive experimental data on properties of persistent spiking neurons in entorhinal cortex (Egorov et al., 2002; Fransén et al., 2006). That implementation uses changes in spiking phase caused by transient input but does not use long-term changes in persistent spiking frequency caused by stronger input.

In most simulations presented here, the model in Equation 1 was replaced with equation 2 that generates denser grid cell firing and more effective place cell formation. This gave the same function as equation 1 with less variability in spike timing.

$$g_{jk}(t)=\Theta[\prod_i \cos(2\pi f_j B \int_0^t \vec{h}_i(\tau)d\tau+\vec{\varphi}_{ik})] \quad (2)$$

These models of grid cells generate grid cell firing patterns that depend on three parameters. The size and spacing of firing fields depends upon parameter f_j, the spatial phase depends upon $\vec{\varphi}_{ik}$, and the orientation depends upon the parameter ϕ_ι (described in the section on head direction input). Examples of grid cell firing activity are shown for random foraging in an open field in Figure 2. For ease of viewing, only 48 cells are shown in Figures 2 and 3. In Figure 3, firing patterns are shown for the same grid cell model during simulated running of a circular track during waking. Grid cell patterns similar to those on the circular track in Figure 3 provided the input for encoding in these simulations. The simulations presented here all used 75 grid cells (25 grid cells at each frequency, with 5 different spatial phases in each spatial dimension).

Note that the function of the model presented here can be obtained with different types of grid cell models, as long as they perform path integration based on head direction activity. Thus, the model can also function with grid cell models using interactions between neurons spiking at different phases (Hasselmo, 2008; Hasselmo and Brandon, 2008), and with continuous attractor models updated by head direction input (Fuhs and Touretzky, 2006; McNaughton et al., 2006).

Place cells

The next stage of the model involves the generation of place cell spiking activity based on grid cell spiking activity. Previous research has proposed different ways by which place cells could arise from grid cell input (Fuhs and Touretzky, 2006; McNaughton et al., 2006; Rolls et al., 2006; Solstad et al., 2006; Franzius et al., 2007b; Molter and Yamaguchi, 2007). The mechanism used here resembles previous models, and was selected for simplicity and

computation speed. In the model presented here, a simple thresholded summation of the location dependent firing properties of entorhinal grid cells is used for the initial induction of place cell activity. A wide array of grid cells with different spatial phases and frequencies are simulated. Place cells are then created during a period before simulation of waking (encoding) and REM replay. During this period, random subsets of three grid cells are selected as inputs for a new place cell that fires in any location where all three grid cells fire. This generates a spatial firing pattern for each place cell that is evaluated by taking the standard deviation of spiking location in the x and y dimension. If the standard deviation of spiking location is smaller than a previously set parameter in both dimensions, then this place cell is selected for inclusion. The input synapses from the randomly selected subset of three grid cells to this place cell are strengthened according to the outer product equation:

$$W_{GP} = \sum \vec{g}\,(t)^T\, \vec{p}\,(t) \tag{3}$$

Where $\vec{g}\,(t)^T$ is a column vector of presynaptic grid cell activity including the three currently selected grid cells, and $\vec{p}\,(t)$ is a row vector of place cell activity with only the currently selected place cell active. This ensures that the same place cells are reliably activated in the same location dependent on the pattern of grid cell spiking induced by the phase of grid cells.

During both waking (encoding) and REM replay, the place cell row vector $\vec{p}\,(t)$ results from the pattern of activity in the grid cell vector $\vec{g}\,(t)$ dependent upon multiplication by the previously modified synaptic connectivity W_{GP} between these regions as follows:

$$\vec{p}\,(t) = \vec{g}\,(t) W_{GP} \tag{4}$$

Examples of individual place cells from the simulation are shown for an open field trajectory in Figure 4A and for the circular track in Figure 4B. The coverage of the circular track by the firing fields of 400 place cells is shown in Figure 4C, illustrating that this number of place cells effectively represents location throughout the circular track. Most simulations presented here used 400 place cells, except where the effect of number of place cells on REM replay is tested.

The responses of the grid cells and place cells in this model are not direction dependent, consistent with data from recordings in the open field. However, if the grid cell oscillation phase is reset at the reward location, the response of grid cells (and therefore also of place cells) will be directional. Alternately, if the grid cell phase is updated by running speed alone without head direction, then the grid cells will respond on the basis of the arc length of the trajectory, rather than two dimensional location. In both of these conditions, if the rat were tested with a different direction of running, the firing pattern of grid cells and place cells would differ. This might enhance the capacity to encode overlapping trajectories without interference (Hasselmo, 2007).

Head direction cell activity

The representation of movement direction (velocity) in the model is provided by head direction cells. Extensive experimental data describes head direction cells in the deep layers of the entorhinal cortex (Sargolini et al., 2006) and in other areas including the postsubiculum (dorsal presubiculum) and the anterior thalamus (Taube et al., 1990a; Knierim et al., 1995; Taube and Burton, 1995; Sharp, 1996; Taube et al., 1996; Knierim et al., 1998; Sharp et al., 2001; Taube and Bassett, 2003; Yu et al., 2006). Head direction cells fire selectively when the rat is heading in angles close to the preferred direction of the cell. In the model, the activity of head direction cells is modulated by the speed of the simulated rat. Physiologically, this could arise from input

from cells showing firing rate changes with translational speed in deep entorhinal layers (Sargolini et al., 2006) and in postsubiculum (Taube et al., 1990b; Sharp, 1996). Alternately, the speed modulation could also arise due to modulation from neurons in other regions that respond linearly to different speeds of translational motion (Sharp, 1996; O'Keefe et al., 1998; Sharp and Turner-Williams, 2005; Sharp et al., 2006).

This model simulates the activity of multiple head direction cells that are modulated by speed. Head direction cell activity is represented by the vector $\vec{h}(t)$. The model computes the speed-modulated head direction response from the velocity vector of movement in space $\vec{v}(t) = [\Delta x(t)\ \Delta y(t)]$ that combines the distance moved in the x and y directions during each discrete unit of time t (20 msec in these simulations). The velocity vector is multipled by the head direction transformation matrix (H) to obtain the speed modulated head direction vector $\vec{h}(t)$:

$$\vec{h}(t) = \vec{v}(t)H = \vec{v}(t)\begin{bmatrix} \cos(\phi_1) & \cos(\phi_2) & \cos(\phi_3) & \\ \sin(\phi_1) & \sin(\phi_2) & \sin(\phi_3) & \cdots \end{bmatrix} \quad (5)$$

The model performs similarly with two different versions of speed modulated head direction input, as used in the Burgess grid cell model (Burgess et al., 2007; Hasselmo et al., 2007). As presented above, Equation 5 produces head direction activity going positive and negative, and the grid cell model in Equations 1 and 2 functions effectively with this input. However, because head direction cells have low background firing and increase their firing in only one direction, the model was also tested with the head direction vector rectified by a threshold linear function (with threshold zero). With this input, the grid cell model was modified to allow interactions of head direction inputs with differences of 180 degrees (Burgess et al., 2007; Hasselmo et al., 2007).

In the matrix H, each value ϕ_i represents the preferred angle of one individual head direction cell. In most simulations, the preferred angles were set at intervals of $\pi/3$ radians (60 degrees) and 6 head direction cells were used. As the velocity vector changes over time $\vec{v}(t)$, this changes the speed modulated head direction vector over time $\vec{h}(t)$. The activity of speed modulated head direction cells in the model is shown in Figure 5. The tuning of two different cells to head direction is shown in Figure 5A. The lines in Figure 5B show the head direction vectors coded by the full population of head direction cells during waking (at every fifth time step for clarity). Here the vectors change systematically with the tangent of the trajectory. The lines in Figure 5C show the head direction vector at every time point during REM replay.

Phases of grid cell oscillations code continuous location

The depolarization of grid cell dendrites by speed modulated head direction input increases dendritic frequency and advances the phase of the dendritic oscillations in the grid cell model. This causes the change in phase of grid cell dendritic oscillations $\vec{\varphi}(t)$ to effectively integrate the speed modulated head direction vector $\vec{h}(t)$, that is proportional to the velocity vector. This means that the two-dimensional spatial location vector $\vec{x}(t) = [x(t)\ y(t)]$ during waking is directly coded by the phase vector of grid cell dendritic oscillations (Hasselmo, 2007; Hasselmo et al., 2007). The dendritic oscillation phase is scaled by the orientation selectivity of the head direction cells (represented by a matrix H) as well as the intrinsic frequency f of the grid cell, and the scaling factor B. The grid cell phase is related to the location vector $\vec{x}(t)$ at each time point relative to the starting location x_0 as follows: $\vec{\varphi}(t) - \varphi_k = (\vec{x}(t) - \vec{x}_0)H2\pi fB$.

Therefore, the coding of two-dimensional location (relative to starting location) by dendritic oscillation phase can be obtained by using the inverse equation:

$$\vec{x}\ (t) - \vec{x}_0 = (\vec{\varphi}\ (t) - \varphi_k) H^{-1} / 2\pi f B. \tag{6}$$

The internal representation of location can be obtained from the phase of just two grid cell dendrites by using the following inverse matrix (Strang, 1988) based on the head direction transform matrix in equation 5:

$$H^{-1} = \begin{bmatrix} \sin\phi_2 & -\sin\phi_1 \\ -\cos\phi_2 & \cos\phi_1 \end{bmatrix} / (\cos\phi_1 \sin\phi_2 - \sin\phi_1 \cos\phi_2) \tag{7}$$

Note that when the rectified version of the transform matrix is used, this requires combining phases before the transform in the same manner that head direction inputs were combined. The inverse transform of grid cell phase is used in Figure 6, 8, 9 and 12 to demonstrate how the activity of grid cells in the model codes continuous spatial location over time during waking, and how the phase of the same grid cells shifts in a systematic way due to temporally structured replay of trajectories during simulated REM sleep. In short, the inverse transform of grid cell phase allows continuous plotting of the internal representation of location during REM replay.

The integration of velocity by phase is sensitive to the accumulation of noise. Some simulations of encoding used random changes in running speed to test noise sensitivity, but the integration of velocity was assumed to be accurate to reduce the complexity of the simulation. Integration noise would require updating of phase by sensory input from the environment, as addressed in previous studies (Burgess et al., 2007; Franzius et al., 2007a).

Encoding during waking

Simulations of waking behavior focus on the rat moving in a circular trajectory over a period of 24 seconds (1200 steps). The movement for each 20 msec time step along this trajectory allows computation of the velocity vector that determines the activity of the head direction vector $\vec{h}\ (t)$ as shown in Equation 5. During waking, the head direction activity is driven by sensory and proprioceptive input via the head direction circuit from brainstem structures through anterior thalamus to the postsubiculum (Goodridge and Taube, 1997; Sharp et al., 2001; Taube and Bassett, 2003). The influence of feedback from hippocampal place cells is modelled as weaker than the influence of excitatory sensory input that dominates head direction activity during waking (possibly due to feedforward inhibition). Neuromodulators could contribute to this difference in dynamics between waking and REM sleep (Hasselmo, 1999). The head direction vector updates the activity of grid cells according to Equation 2. As the virtual rat moves, the grid cell activity shifts and causes sequential activation of different place cells via synaptic connections according to Equation 4.

Encoding of the behavior during waking results from synaptic modification of the connections W_{PH} between the full population of place cells $\vec{p}\ (t)$ and the population of head direction cells $\vec{h}\ (t)$, as follows:

$$W_{PH}(t+1) = (W_{PH}(t) + \sum_t \vec{p}\ (t)^T\ \vec{h}\ (t))/2 \tag{8}$$

This equation updates the weights by the average of the previous weight and the outer product of the current place cell $\vec{p}\ (t)$ and head direction vector $\vec{h}\ (t)$. This synaptic modification provides the mechanism for later retrieval of movements associated with each place along the trajectory, but does not influence head direction activity during waking. Because the equation for synaptic

modification depresses some connections while enhancing others, the initial pattern of connectivity has little effect. Most simulations started with W_{PH} as a matrix of zeros, but similar performance occurred during testing of a wide range of starting values. This matrix could correspond to direct projections from region CA1 of the hippocampus to the postsubiculum (van Groen and Wyss, 1990), or to the effect of projections from hippocampus to subiculum (Swanson et al., 1978; Amaral and Witter, 1989), and projections from the subiculum to the postsubiculum and medial entorhinal cortex (Naber and Witter, 1998)

Temporally structured replay during REM sleep

During simulation of REM sleep, the network receives no direct sensory input. The network is only presented the initial pattern of grid cell, place cell and head direction activity on the first step that starts the replay. After this initial cue, the activity of head direction cells is determined entirely by the spread of activity across previously modified synapses W_{PH} from the hippocampus, and not by the input present during waking. For each new pattern of place cell activation, activity spreads across the connections W_{PH} to activate the associated head direction vector. The spread of activity from place cells to head direction cells is summarized by the following equation, which includes normalization based on the sum of all place cell activity.

$$\vec{h}\ (t) = \vec{p}\ (t) W_{PH} / \sum \vec{p}\ (t) \tag{9}$$

During REM replay, this head direction vector then causes a progressive shift in the phase of grid cell oscillations (Equation 2) and a shift in the pattern of grid cell firing until spiking is induced in a new set of place cells (Equation 4). If the transition to new place cell input is slow, the head direction vector is maintained by graded persistent firing of the head direction cells. Graded persistent firing has been shown in intracellular recording from neurons in deep layers of entorhinal cortex slice preparations (Egorov et al., 2002; Fransén et al., 2006) and persistent firing has been shown with whole cell patch recording in slices of postsubiculum (Yoshida and Hasselmo, 2008). These data on persistent spiking were observed in the presence of cholinergic agonists, indicating that these effects would be present during the high levels of acetylcholine present in cortical structures during REM sleep (Marrosu et al., 1995). Thus, if necessary, the persistent firing allows head direction activity to continue for a period of time during which it causes a shift in frequency of oscillations in entorhinal grid cells.

The head direction vector causes a progressive shift in the phase of grid cell oscillations and a shift in the pattern of grid cell firing until spiking is induced in a new set of place cells. The new place cell activity then induces a new pattern of head direction firing $\vec{h}\ (t)$ according to Equation 9 that further updates the pattern of grid cell activity, and the cycle of temporally structured replay continues. Thus, continuous REM replay depends upon interactions in a loop including connections from place cells $\vec{p}\ (t)$ to head direction cells $\vec{h}\ (t)$, from head direction cells $\vec{h}\ (t)$ to grid cells $\vec{g}\ (t)$ and from grid cells back to place cells $\vec{p}\ (t)$.

RESULTS

In these simulations, interacting populations of grid cells, place cells and head direction cells encode the circular trajectory through the environment experienced during waking, and demonstrate temporally structured replay of the activity during simulated REM sleep, as summarized in Figures 5–12.

The temporally structured replay depends upon the spatial pattern of activity of different populations that are shown in Figures 2–5. The spiking activity that occurs in the population

of grid cells in the model is shown during running in an open field environment in Figure 2. The pattern of spiking activity in this population of grid cells effectively replicates the firing properties of grid cells recorded in medial entorhinal cortex during random foraging in an open field (Hafting et al., 2005;Sargolini et al., 2006;Fyhn et al., 2007). The properties of the different grid cells shown in Figure 2 are influenced by the oscillatory phase φ_{ik} that determines the spatial phase of grid cell firing in two dimensions, and by the parameter of baseline oscillation frequency f_j that determines the size and spacing of firing fields.

Figure 3 shows the pattern of firing of these grid cells during running on the circular track that is the primary focus of these simulations. Note that each grid cell shows multiple different firing fields on the circular track. The grid cell firing results from progressive input from head direction cells firing in response to progressively different head directions at different positions around the circle, as shown in Figure 5A.

Individual cells in the population of place cells in the model replicate the highly localized firing fields of hippocampal place cells, as shown in Figure 4 for an open field trajectory (Figure 4A) and the circular track (Figure 4B). The patterns of grid cell firing spread across the modified synapses W_{GP} from grid cells to place cells. The mechanism for initial selection of place cells results in connectivity from groups of grid cells with overlapping firing locations to result in the individual examples of localized place cell firing shown in Figures 4A and 4B. The full set of 400 place cells effectively codes locations around most of the circular track, as shown by the plot in Figure 4C showing spiking activity of all place cells in the population.

Individual head direction cells in the model respond when the rat moves in directions close to the preferred direction of the cell, as shown in Figure 5(A). These tuning curves resemble the data on cells with relatively wide tuning to head direction (Sharp, 1996; Sargolini et al., 2006). During running on the circular track in the waking period, the head direction cells show a progressive change in firing driven by the different head directions of the virtual rat as it runs, as shown in Figure 5B. During REM sleep, the head direction cell activity is driven by the spread of activity across previously modified synapses W_{PH}. The retrieval mechanism causes progressive activation in the population of head direction cells that codes different directions of movement, as shown in Figure 5C. During REM sleep, the retrieval mechanism does not run as smoothly as the input during waking, resulting in more variability in the direction and magnitude of the vectors representing head direction activity in Figure 5C. However, this variability does not prevent effective retrieval function, and REM replay is similar even if noise is added to the head direction vectors during waking (encoding).

The progressive shift in activation of different head direction cells during the REM retrieval phase results in a systematic structured change in the phase of oscillations in simulated entorhinal grid cells, as shown in Figure 6. The trajectory experienced during waking is shown in Figure 6A. The inverse transform of the grid cell phase in Equations 6 and 7 is used to plot the internal representation of location over time during REM sleep. As shown in Figure 6B, the internal representation of location (black line) follows a trajectory through space that effectively matches the trajectory experienced during waking (Figure 6A). There is some variation in the trajectory during different retrieval examples (see Figure 8), but the network is usually able to effectively retrieve the full trajectory.

Most simulations set the initial conditions of replay to match the pattern of grid cell, place cell and head direction activity from the start of the waking encoding period. However, the network can perform replay with any initial conditions for head direction cells because the head direction activity during REM is determined by the synaptic input from place cells. In addition, the network can perform replay with any initial conditions for place cell activity because this activity is rapidly altered by the current grid cell input. Thus, the crucial initial conditions were

determined by the grid cell phase. REM replay occurred for starting grid cell phases corresponding to locations experienced anywhere on the circular track. If the starting grid cell phase did not correspond to a location on the track, then the circuit of place cells and head direction cells was not activated, and the retrieval would drift randomly (unless it happened to overlap with a segment of the circular track).

Examples of the temporally structured replay of place cell activity during different simulations are shown in Figures 7 and 8. Individual simulations differ because of the random selection of grid to place connections. Figure 7 shows activity from one simulation in the form of ten place cells randomly selected from the full population of 400 place cells. The figure shows separate plots for place cell activity during simulated waking behavior (Figure 7A) and during simulated REM sleep (Figure 7B). During the 24 second simulated waking period, the pattern of place cell spiking activity is determined by the trajectory of actual movement through the environment. The virtual rat goes around the circular track four times, resulting in four cycles of sequential activation in the same set of 10 place cells. During simulated REM sleep, the network starts with place cell activity in one location and this triggers four cycles of retrieval of the full circular trajectory. Due to the internal spread of retrieval activity, the network shows sequential place cell activity with spike timing similar to waking.

Figure 8 shows place cell activity during waking behavior and during simulated REM sleep for ten different simulations run separately with creation of different connectivity between grid cells and place cells for each simulation. Each row of the figure shows activity for a different simulation. Each box in column A shows spiking of ten place cells during waking, and the box in the same row of column B shows spiking of the same ten place cells during REM. Column C shows the inverse transform of grid cell phase indicating internal representation of location. In 6 out of 10 cases, the pattern of place cell spiking during the full duration of REM replay closely resembles the pattern of spiking during waking. In these cases, the pattern of place cell spiking during REM shows the same temporal structure as the pattern of place cell spiking during waking.

In some cases, REM replay does not complete multiple cycles. This is consistent with the fact that replay is variable in experimental data. For instance, in the examples in row 3 and 7, REM replay breaks down after one cycle of successful retrieval. This is also visible in the trajectory plots in rows 3 and 7 of column C. In Row 6, REM replay completes three cycles but then ceases. In Row 4, the internal representation during REM replay does not follow the circular track perfectly but still completes all cycles, activating a subset of the place cells activated during waking. In multiple groups of 10 simulations, an average of 6 out of 10 simulations showed successful completion of all cycles. The variation between different simulations results from the random selection of different place cells and the corresponding variation in distribution of synaptic weights between grid cells and place cells and between place cells and head direction cells. The consistency of retrieval could be enhanced by various techniques; for example, associating place with angular velocity, or including cells responding to arc length (Hasselmo, 2007). However, the experimental data also shows variability, and the features of this model could be evaluated by comparing properties of variance in the model with properties of variance in future experimental data.

The speed of temporally structured replay of place cell activity depends upon the magnitude of persistent firing in the head direction cells during REM replay, which is determined by the strength of connections W_{PH} from place cells to head direction cells. This can be demonstrated by altering the strength of W_{PH} by multiplying the matrix with a constant s with different values, as shown in Figures 9 and 10. As shown in Figure 9, multiplying with s=0.5 results in replay that is half the speed of waking (2 cycles are completed during REM replay rather than four). Multiplying with s=1.5 results in replay that is 50 percent faster than waking (6 cycles versus

four). Setting s close to zero greatly slows the sequential activity. The replay can be graded to a range of different speeds as shown in Figure 10. In these figures, simulations with multiple cycles of successful replay were chosen for each value of s. Thus, the model predicts that faster replay corresponds to stronger synaptic connections from place cells to head direction cells, and higher firing rates in head direction cells. Previous studies have demonstrated how difficult it is to show learning-induced changes in synaptic strength (Moser et al., 1993), but unit recording can test the prediction that higher head direction firing rates should be correlated with faster replay.

The temporal structure of replay can even account for changes in the movement speed of the rat during waking. As shown in Figure 11, the simulation shows REM replay of a consistent change in running speed occurring near the reward location during waking. Figure 11A1 shows plots of the running speed (labelled "s") of the virtual rat in cm/sec as well as one dimension of location (labelled "x") in cm. In Fig. 11A1, the location x changes cyclically similar to a sine wave, as the rat runs around the circular track. Speed starts out as a straight line at 50 cm/sec and then reduces to 5 cm/sec near the reward location. In Figure 11A2, there is no external influence on movement. The speed of movement is determined entirely by the spread of activity from place cells to head direction cells. In this case, REM replay still shows the same pattern as waking, with slowing of running speed to about 5 cm/sec near reward location. Figure 11A4 shows that the pattern of place cell activity during REM replay matches that seen during waking (Fig. 11A3), with a longer period of place cell activity during slowing.

REM replay is not altered by noise added to the running speed, as shown in Figure 11(B). In this figure, random changes in running speed were added in proportion to 30% of total running speed. This does not prevent the REM replay in Fig. 11B2 from showing the same pattern of location and speed changes that appear during waking in Fig. 11B1. Performance was similar if speed was assumed uniform but noise was added at the stage of the speed-modulated head direction activity. Note that this example shows a reduction of running speed to 25 cm/sec during waking and REM replay, to illustrate the capacity to match different quantitative changes in running speed. Note that noise results in changes in running speed that are recapitulated during each cycle of REM replay. Figure 11C shows that the REM replay also replicates changes in the baseline running speed from 50 cm/sec to 25 cm/sec (note the increase in simulation period to 48 seconds).

As noted above, the speed of REM replay depends upon the magnitude of synaptic transmission on the synapses W_{PH} from place cells to head direction cells. Systematic changes in strength due to a multiplier of W_{PH} cause systematic changes in number of cycles during replay, as shown in Figure 12A. The success of retrieval also depends upon the number of place cells used in the network, as shown in Figure 12B. This figure shows the average number of cycles of REM replay for 10 simulations run with different numbers of place cells (and with noise set at 20%). The waking period was 24 seconds, but each simulation was tested for the number of cycles during a longer period of 48 seconds of REM replay. For small numbers of place cells (e.g. between 36 and 256 place cells), there was less than one cycle of REM replay in the majority of cases, and the mean number of cycles completed was less than two. In contrast, for larger numbers of place cells (e.g. 324 and higher), the average number of cycles of REM replay jumps up to over three cycles, indicating successful REM replay of multiple cycles in most simulations. This shows that when a sufficient number of place cells provide a high resolution representation of place in the environment, the network performs successful REM replay of multiple cycles of the task.

These simulations propose a potential mechanism for REM replay in place cells, and generate predictions that REM replay should appear in other populations of cells, including both head direction cells and grid cells, with specific timing in coordination with the place cell activity.

As shown in Figure 12C, this model predicts that entorhinal grid cells should show patterns of activity during REM sleep that correlate with the patterns of activity present during waking behaviour. Figure 12C5 shows that the pattern of grid cell activity during simulated REM closely resembles the pattern of grid cell activity induced by running on the circular track during waking, as shown in Figure 12C4. Thus, these simulations generate detailed predictions about the expected pattern of spiking activity during REM replay.

DISCUSSION

The simulations presented here show how temporally structured replay during REM sleep (Louie and Wilson, 2001) could arise from a circuit including grid cells, place cells and head direction cells. Place cells in the simulation respond to the circular trajectory during waking (Figure 7A and Figure 8A), and the same place cells are activated sequentially in the absence of sensory input during the simulation of REM replay (Figure 7B and Figure 8B). The sequential readout of place cell activity during simulated REM sleep matches the timing of place cell activity during waking, including changes in the speed of movement (Figure 11). The inverse transform of grid cell phase shows that the internal representation of the trajectory during simulated REM sleep closely matches the trajectory experienced during waking (Figure 6, 8 and 9).

These simulations demonstrate a potential mechanism for the temporally structured replay of place cell activity during REM sleep demonstrated experimentally using multiple single unit recording in rats (Louie and Wilson, 2001). Similar to the data, the simulation shows REM replay with temporal scaling similar to waking activity. Changes in the strength of synaptic connections between place cells and head direction cells (Figure 9 and 10) alter the speed of REM replay relative to waking in a manner that resembles the variability in scaling factor seen in the data for different REM episodes (Louie and Wilson, 2001).

The model presented here generates the prediction that head direction activity should show a corresponding replay of sequences occurring during waking. This prediction of the model motivated experiments that show head direction cell activity during REM sleep that correlates with prior waking behavior (Brandon et al., 2008). The model also generates the prediction that grid cell activity in entorhinal cortex should show replay of particular sequences occurring during waking (Figure 12).

This model could function with any of a wide range of different grid cell models (Fuhs and Touretzky, 2006; McNaughton et al., 2006; Blair et al., 2007; Burgess et al., 2007), as long as they perform path integration based on head direction and speed. The simulations shown here used grid cell activity based on a previously published model of medial entorhinal grid cells (Burgess et al., 2005; O'Keefe and Burgess, 2005; Burgess et al., 2007) based on earlier models of theta phase precession (O'Keefe and Recce, 1993; Lengyel et al., 2003). In this model, input from different head direction cells to single entorhinal grid cells alters the frequency and phase of dendritic oscillations relative to each other, resulting in an interference pattern that replicates grid cell firing (Burgess et al., 2007; Hasselmo et al., 2007). As shown in Figures 2 and 3, the model produces grid cells with different properties of field spacing and size that depend upon the baseline oscillation frequency within each neuron. The grid cell firing corresponds to differences in field spacing and size seen along the dorsal to ventral axis of medial entorhinal cortex (Hafting et al., 2005; Sargolini et al., 2006; Fyhn et al., 2007), and the oscillation frequency difference corresponds to the experimental data showing membrane potential oscillation differences along the dorsal to ventral axis of medial entorhinal cortex (Giocomo et al., 2007; Hasselmo et al., 2007). The same circuit presented here could function with other models of grid cells, including models using network attractor dynamics updated by head direction input (Fuhs and Touretzky, 2006; McNaughton et al., 2006). This grid cell model is

mathematically similar to a grid cell model created using the mechanism of persistent firing (Hasselmo, 2008; Hasselmo and Brandon, 2008) in which grid cell firing arises from convergent input from persistent spiking neurons with specific phase relationships determined by head direction.

The simulation presented here could function with a range of mechanisms for creating place cells from grid cell input (Fuhs and Touretzky, 2006; McNaughton et al., 2006; Rolls et al., 2006; Solstad et al., 2006; Franzius et al., 2007b; Molter and Yamaguchi, 2007). The mechanism presented here selects place cells with spatial variance below a chosen value and strengthens synaptic input to these place cells from medial entorhinal grid cells. The size of place cell firing fields necessary for effective function in the model are consistent with evidence for the size of place cell firing fields in the hippocampus.

The most specific requirements of the model presented here concern the nature of head direction responses and the influence of place cells on head direction cells. Extensive experimental data describes head direction cells in areas receiving output from the hippocampal formation, including the deep layers of the entorhinal cortex (Sargolini et al., 2006) and the postsubiculum (dorsal presubiculum) (Taube et al., 1990a; Knierim et al., 1995; Taube and Burton, 1995; Sharp, 1996; Taube et al., 1996; Sharp et al., 2001; Taube and Bassett, 2003). The influence of place cells on head direction cells could underlie data showing cells with a combination of place and head direction dependence in the presubiculum and parasubiculum (Cacucci et al., 2004). The head direction tuning width used here matches data on cells with relatively wide head direction tuning (Sharp, 1996; Sargolini et al., 2006), but narrower tuning could be used with a different grid cell model. The current simulation uses head direction activity modulated by movement speed. Some neurons show speed modulation in deep entorhinal cortex (Sargolini et al., 2006), postsubiculum (Taube et al., 1990b; Sharp, 1996) and related structures (O'Keefe et al., 1998; Sharp and Turner-Williams, 2005; Sharp et al., 2006). However, this aspect of the circuit might require activation of separate populations of cells that then converge on the grid cell representation.

Because head direction cells are also seen in retrospenial cortex (Cho and Sharp, 2001), the reactivation of head direction cells during retrieval could underlie evidence for activation of retrosplenial cortex in humans during performance of autobiographical memory tasks (Piefke et al., 2003; Steinvorth et al., 2006) and spatial memory tasks (Epstein et al., 2007; Iaria et al., 2007).

The oscillatory dynamics used in the grid cell model are consistent with the theta frequency field potential oscillations that appear prominently in layers of the hippocampus where synaptic input arrives from the entorhinal cortex (Brankack et al., 1993; Booth and Poe, 2006; Hasselmo et al., 2007), and with differences in intrinsic frequency of neurons along the dorsal to ventral axis of hippocampus (Maurer et al., 2005).

If the same location in the environment is associated with multiple different head directions or speeds, this can cause ambiguity for replay. This ambiguity can be overcome by neural activity dependent upon the trajectory arc length or temporal duration from a recent stopping point. Arc length coding can be obtained in the model by resetting oscillatory phase at stopping locations (Hasselmo, 2007; Hasselmo, 2008) and removing the influence of head direction by using input from cell modulated by speed alone (Sharp, 1996; O'Keefe et al., 1998; Sharp et al., 2006). The simulation of arc-length coding (Hasselmo, 2007) closely matches spiking properties of hippocampal neurons that respond selectively dependent on recent context in tasks such as spatial alternation (Lee et al., 2006) and delayed non-match to position (Griffin et al., 2007).

If the influence of external sensory input is reduced for a period during waking, the circuit presented here could perform episodic retrieval of previously experienced trajectories during waking. This could underlie data on forward replay of place cell activity corresponding to experienced trajectories shown experimentally during waking behavior (Foster and Wilson, 2006; Diba and Buzsaki, 2007; Johnson and Redish, 2007). The model does not address reverse replay of sequences, but this reverse replay has not been demonstrated during REM sleep replay (Louie and Wilson, 2001). With appropriate increases in replay speed, this circuit could also underlie forward hippocampal replay occurring during slow wave sleep (Skaggs and McNaughton, 1996; Nadasdy et al., 1999) that could drive the replay shown in neocortical structures (Ribeiro et al., 2004; Euston et al., 2007; Ji and Wilson, 2007). However, the faster time scale of replay in these other studies would require a stronger influence of place cells on head direction cells, or an increase in oscillation frequencies in entorhinal cortex. Faster replay could also be due to direct associations between place cells coding states, rather than the slower mechanisms of state to action association used here for temporally structured replay.

The sequence replay mechanisms simulated here could prove important both for consolidation of trajectories in the environment and for episodic retrieval of trajectories. Experimental data supports an important role of the hippocampus in learning the sequential order of events or stimuli in the environment (Eichenbaum et al., 1999). This could involve association of elements of a trajectory with individual events or stimuli. Lesions of the hippocampus impair the ability to learn and disambiguate non-spatial sequences such as a sequence of odors in a sequential discrimination task (Agster et al., 2002) and impair the ability to retrieve information about the order of stimuli (Fortin et al., 2002; Kesner et al., 2002). In addition, lesions of the hippocampus impair performance in spatial tasks requiring memory for the previous spatial trajectory performed within a task (Ennaceur et al., 1996; Ainge et al., 2007). Performance in tasks requiring memory for spatial trajectories is also impaired by lesions of the entorhinal cortex (Steffenach et al., 2005) and the postsubiculum (Taube et al., 1992; Calton et al., 2003), indicating the importance of the other components of the circuit simulated in this paper. The impairments caused by these lesions could be related to loss of the ability to encode and retrieve temporally structured sequences of activity.

Acknowledgements

I appreciate comments on the text from Mark P. Brandon. Research supported by Silvio O. Conte Center grant NIMH MH71702, NIMH R01 MH60013, NIMH R01 MH61492, NIMH MH60450, NSF SLC SBE 0354378 and NIDA R01 DA16454 (part of the CRCNS program).

References

Agster KL, Fortin NJ, Eichenbaum H. The hippocampus and disambiguation of overlapping sequences. J Neurosci 2002;22:5760–5768. [PubMed: 12097529]

Ainge JA, van der Meer MA, Langston RF, Wood ER. Exploring the role of context-dependent hippocampal activity in spatial alternation behavior. Hippocampus 2007;17:988–1002. [PubMed: 17554771]

Alonso A, Llinas RR. Subthreshold Na-dependent theta-like rhythmicity in stellate cells of entorhinal cortex layer II. Nature 1989;342:175–177. [PubMed: 2812013]

Alonso A, Klink R. Differential electroresponsiveness of stellate and pyramidal-like cells of medial entorhinal cortex layer II. J Neurophysiol 1993;70:128–143. [PubMed: 8395571]

Amaral DG, Witter MP. The 3-dimensional organization of the hippocampal formation - A review of anatomical data. Neurosci 1989;31:571–591.

Blair HT, Welday AC, Zhang K. Scale-invariant memory representations emerge from moire interference between grid fields that produce theta oscillations: a computational model. J Neurosci 2007;27:3211–3229. [PubMed: 17376982]

Booth V, Poe GR. Input source and strength influences overall firing phase of model hippocampal CA1 pyramidal cells during theta: relevance to REM sleep reactivation and memory consolidation. Hippocampus 2006;16:161–173. [PubMed: 16411243]

Brandon MP, Andrews CM, Hasselmo ME. Postsubicular neural activity during REM sleep shows replay of head direction activity during waking. Soc Neurosci Abstr. 2008in press

Brankack J, Stewart M, Fox SE. Current source density analysis of the hippocampal theta rhythm: associated sustained potentials and candidate synaptic generators. Brain Research 1993;615:310–327. [PubMed: 8364740]

Burgess N, Barry C, O'Keefe J. An oscillatory interference model of grid cell firing. Hippocampus 2007;17:801–812. [PubMed: 17598147]

Burgess, N.; Barry, C.; Jeffery, KJ.; O'Keefe, J. A grid and place cell model of path integration utilizing phase precession versus theta. Computational Cognitive Neuroscience Meeting. Computational Cognitive Neuroscience Meeting; Washington, D.C.. 2005.

Caballero-Bleda M, Witter MP. Regional and laminar organization of projections from the presubiculum and parasubiculum to the entorhinal cortex: an anterograde tracing study in the rat. J Comp Neurol 1993;328:115–129. [PubMed: 8429124]

Cacucci F, Lever C, Wills TJ, Burgess N, O'Keefe J. Theta-modulated place-by-direction cells in the hippocampal formation in the rat. J Neurosci 2004;24:8265–8277. [PubMed: 15385610]

Calton JL, Stackman RW, Goodridge JP, Archey WB, Dudchenko PA, Taube JS. Hippocampal place cell instability after lesions of the head direction cell network. J Neurosci 2003;23:9719–9731. [PubMed: 14585999]

Cho J, Sharp PE. Head direction, place, and movement correlates for cells in the rat retrosplenial cortex. Behav Neurosci 2001;115:3–25. [PubMed: 11256450]

Diba K, Buzsaki G. Forward and reverse hippocampal place-cell sequences during ripples. Nat Neurosci 2007;10:1241–1242. [PubMed: 17828259]

Dickson CT, Magistretti J, Shalinsky MH, Fransen E, Hasselmo ME, Alonso A. Properties and role of I (h) in the pacing of subthreshold oscillations in entorhinal cortex layer II neurons. J Neurophysiol 2000;83:2562–2579. [PubMed: 10805658]

Egorov AV, Hamam BN, Fransen E, Hasselmo ME, Alonso AA. Graded persistent activity in entorhinal cortex neurons. Nature 2002;420:173–178. [PubMed: 12432392]

Eichenbaum H, Dudchenko P, Wood E, Shapiro M, Tanila H. The hippocampus, memory, and place cells: is it spatial memory or a memory space? Neuron 1999;23:209–226. [PubMed: 10399928]

Ennaceur A, Neave N, Aggleton JP. Neurotoxic lesions of the perirhinal cortex do not mimic the behavioural effects of fornix transection in the rat. Behav Brain Res 1996;80:9–25. [PubMed: 8905124]

Epstein RA, Parker WE, Feiler AM. Where am I now? Distinct roles for parahippocampal and retrosplenial cortices in place recognition. J Neurosci 2007;27:6141–6149. [PubMed: 17553986]

Euston DR, Tatsuno M, McNaughton BL. Fast-forward playback of recent memory sequences in prefrontal cortex during sleep. Science 2007;318:1147–1150. [PubMed: 18006749]

Fortin NJ, Agster KL, Eichenbaum HB. Critical role of the hippocampus in memory for sequences of events. Nature Neuroscience 2002;5:458–462.

Foster DJ, Wilson MA. Reverse replay of behavioural sequences in hippocampal place cells during the awake state. Nature 2006;440:680–683. [PubMed: 16474382]

Fransén E, Tahvildari B, Egorov AV, Hasselmo ME, Alonso AA. Mechanism of graded persistent cellular activity of entorhinal cortex layer v neurons. Neuron 2006;49:735–746. [PubMed: 16504948]

Franzius M, Sprekeler H, Wiskott L. Slowness and sparseness lead to place, head-direction, and spatial-view cells. PLoS Comput Biol 2007a;3:e166. [PubMed: 17784780]

Franzius M, Vollgraf R, Wiskott L. From grids to places. J Comput Neurosci 2007b;22:297–299. [PubMed: 17195112]

Fuhs MC, Touretzky DS. A spin glass model of path integration in rat medial entorhinal cortex. J Neurosci 2006;26:4266–4276. [PubMed: 16624947]

Fyhn M, Hafting T, Treves A, Moser MB, Moser EI. Hippocampal remapping and grid realignment in entorhinal cortex. Nature 2007;446:190–194. [PubMed: 17322902]

Giocomo LM, Zilli EA, Fransen E, Hasselmo ME. Temporal frequency of subthreshold oscillations scales with entorhinal grid cell field spacing. Science 2007;315:1719–1722. [PubMed: 17379810]

Goodridge JP, Taube JS. Interaction between the postsubiculum and anterior thalamus in the generation of head direction cell activity. J Neurosci 1997;17:9315–9330. [PubMed: 9364077]

Griffin AL, Eichenbaum H, Hasselmo ME. Spatial representations of hippocampal CA1 neurons are modulated by behavioral context in a hippocampus-dependent memory task. J Neurosci 2007;27:2416–2423. [PubMed: 17329440]

Hafting T, Fyhn M, Molden S, Moser MB, Moser EI. Microstructure of a spatial map in the entorhinal cortex. Nature 2005;436:801–806. [PubMed: 15965463]

Hasselmo ME. Neuromodulation: acetylcholine and memory consolidation. Trends Cogn Sci 1999;3:351–359. [PubMed: 10461198]

Hasselmo ME. Arc length coding by interference of theta frequency oscillations may underlie context-dependent hippocampal unit data and episodic memory function. Learn Mem 2007;14:782–794. [PubMed: 18007021]

Hasselmo ME. Grid cell mechanisms and function: Contributions of entorhinal persistent spiking and phase resetting. Hippocampus 2008;28:1301–1315.

Hasselmo ME, Eichenbaum H. Hippocampal mechanisms for the context-dependent retrieval of episodes. Neural Netw 2005;18:1172–1190. [PubMed: 16263240]

Hasselmo ME, Brandon MA. Linking cellular mechanisms to behaviour: Entorhinal persistent spiking and membrane potential oscillations may underlie path integration, grid cell firing and episodic memory. Neural Plasticity 2008;2008:658323. [PubMed: 18670635]

Hasselmo ME, Giocomo LM, Zilli EA. Grid cell firing may arise from interference of theta frequency membrane potential oscillations in single neurons. Hippocampus 2007;17:1252–1271. [PubMed: 17924530]

Iaria G, Chen JK, Guariglia C, Ptito A, Petrides M. Retrosplenial and hippocampal brain regions in human navigation: complementary functional contributions to the formation and use of cognitive maps. Eur J Neurosci 2007;25:890–899. [PubMed: 17298595]

Jensen O, Lisman JE. Hippocampal CA3 region predicts memory sequences: accounting for the phase precession of place cells. Learning and Memory 1996a;3:279–287. [PubMed: 10456097]

Jensen O, Lisman JE. Theta/gamma networks with slow NMDA channels learn sequences and encode episodic memory: role of NMDA channels in recall. Learning and Memory 1996b;3:264–278. [PubMed: 10456096]

Ji D, Wilson MA. Coordinated memory replay in the visual cortex and hippocampus during sleep. Nat Neurosci 2007;10:100–107. [PubMed: 17173043]

Johnson A, Redish AD. Neural ensembles in CA3 transiently encode paths forward of the animal at a decision point. J Neurosci 2007;27:12176–12189. [PubMed: 17989284]

Kesner RP, Gilbert PE, Barua LA. The role of the hippocampus in memory for the temporal order of a sequence of odors. Behav Neurosci 2002;116:286–290. [PubMed: 11996313]

Knierim JJ, Kudrimoti HS, McNaughton BL. Place cells, head direction cells, and the learning of landmark stability. J Neurosci 1995;15:1648–1659. [PubMed: 7891125]

Knierim JJ, Kudrimoti HS, McNaughton BL. Interactions between idiothetic cues and external landmarks in the control of place cells and head direction cells. J Neurophysiol 1998;80:425–446. [PubMed: 9658061]

Lee AK, Wilson MA. Memory of sequential experience in the hippocampus during slow wave sleep. Neuron 2002;36:1183–1194. [PubMed: 12495631]

Lee I, Rao G, Knierim JJ. A double dissociation between hippocampal subfields: differential time course of CA3 and CA1 place cells for processing changed environments. Neuron 2004a;42:803–815. [PubMed: 15182719]

Lee I, Yoganarasimha D, Rao G, Knierim JJ. Comparison of population coherence of place cells in hippocampal subfields CA1 and CA3. Nature 2004b;430:456–459. [PubMed: 15229614]

Lee I, Griffin AL, Zilli EA, Eichenbaum H, Hasselmo ME. Gradual translocation of spatial correlates of neuronal firing in the hippocampus toward prospective reward locations. Neuron 2006;51:639–650. [PubMed: 16950161]

Lengyel M, Szatmary Z, Erdi P. Dynamically detuned oscillations account for the coupled rate and temporal code of place cell firing. Hippocampus 2003;13:700–714. [PubMed: 12962315]

Levy WB. A sequence predicting CA3 is a flexible associator that learns and uses context to solve hippocampal-like tasks. Hippocampus 1996;6:579–590. [PubMed: 9034847]

Louie K, Wilson MA. Temporally structured replay of awake hippocampal ensemble activity during rapid eye movement sleep. Neuron 2001;29:145–156. [PubMed: 11182087]

Marrosu F, Portas C, Mascia MS, Casu MA, Fa M, Giagheddu M, Imperato A, Gessa GL. Microdialysis measurement of cortical and hippocampal acetylcholine release during sleep-wake cycle in freely moving cats. Brain Res 1995;671:329–332. [PubMed: 7743225]

Maurer AP, Vanrhoads SR, Sutherland GR, Lipa P, McNaughton BL. Self-motion and the origin of differential spatial scaling along the septo-temporal axis of the hippocampus. Hippocampus 2005;15:841–852. [PubMed: 16145692]

McNaughton BL, Battaglia FP, Jensen O, Moser EI, Moser MB. Path integration and the neural basis of the 'cognitive map'. Nat Rev Neurosci 2006;7:663–678. [PubMed: 16858394]

Molter C, Yamaguchi Y. Impact of temporal coding of presynaptic entorhinal cortex grid cells on the formation of hippocampal place fields. Neural Netw. 2007

Moser E, Mathiesen I, Andersen P. Association between brain temperature and dentate field potentials in exploring and swimming rats. Science 1993;259:1324–1326. [PubMed: 8446900]

Naber PA, Witter MP. Subicular efferents are organized mostly as parallel projections: a double-labeling, retrograde-tracing study in the rat. J Comp Neurol 1998;393:284–297. [PubMed: 9548550]

Nadasdy Z, Hirase H, Czurko A, Csicsvari J, Buzsaki G. Replay and time compression of recurring spike sequences in the hippocampus. J Neurosci 1999;19:9497–9507. [PubMed: 10531452]

O'Keefe J. Place units in the hippocampus of the freely moving rat. Exp Neurol 1976;51:78–109. [PubMed: 1261644]

O'Keefe J, Recce ML. Phase relationship between hippocampal place units and the EEG theta rhythm. Hippocampus 1993;3:317–330. [PubMed: 8353611]

O'Keefe J, Burgess N. Dual phase and rate coding in hippocampal place cells: theoretical significance and relationship to entorhinal grid cells. Hippocampus 2005;15:853–866. [PubMed: 16145693]

O'Keefe J, Burgess N, Donnett JG, Jeffery KJ, Maguire EA. Place cells, navigational accuracy, and the human hippocampus. Philos Trans R Soc Lond B Biol Sci 1998;353:1333–1340. [PubMed: 9770226]

Piefke M, Weiss PH, Zilles K, Markowitsch HJ, Fink GR. Differential remoteness and emotional tone modulate the neural correlates of autobiographical memory. Brain 2003;126:650–668. [PubMed: 12566286]

Ribeiro S, Gervasoni D, Soares ES, Zhou Y, Lin SC, Pantoja J, Lavine M, Nicolelis MA. Long-lasting novelty-induced neuronal reverberation during slow-wave sleep in multiple forebrain areas. PLoS Biol 2004;2:E24. [PubMed: 14737198]

Rolls ET, Stringer SM, Elliot T. Entorhinal cortex grid cells can map to hippocampal place cells by competitive learning. Network 2006;17:447–465. [PubMed: 17162463]

Sargolini F, Fyhn M, Hafting T, McNaughton BL, Witter MP, Moser MB, Moser EI. Conjunctive representation of position, direction, and velocity in entorhinal cortex. Science 2006;312:758–762. [PubMed: 16675704]

Sharp PE. Multiple spatial/behavioral correlates for cells in the rat postsubiculum: multiple regression analysis and comparison to other hippocampal areas. Cereb Cortex 1996;6:238–259. [PubMed: 8670654]

Sharp PE, Turner-Williams S. Movement-related correlates of single-cell activity in the medial mammillary nucleus of the rat during a pellet-chasing task. J Neurophysiol 2005;94:1920–1927. [PubMed: 15857969]

Sharp PE, Blair HT, Cho J. The anatomical and computational basis of the rat head-direction cell signal. Trends Neurosci 2001;24:289–294. [PubMed: 11311382]

Sharp PE, Turner-Williams S, Tuttle S. Movement-related correlates of single cell activity in the interpeduncular nucleus and habenula of the rat during a pellet-chasing task. Behav Brain Res 2006;166:55–70. [PubMed: 16143407]

Skaggs WE, McNaughton BL. Replay of neuronal firing sequences in rat hippocampus during sleep following spatial experience. Science 1996;271:1870–1873. [PubMed: 8596957]

Solstad T, Moser EI, Einevoll GT. From grid cells to place cells: a mathematical model. Hippocampus 2006;16:1026–1031. [PubMed: 17094145]

Steffenach HA, Witter M, Moser MB, Moser EI. Spatial memory in the rat requires the dorsolateral band of the entorhinal cortex. Neuron 2005;45:301–313. [PubMed: 15664181]

Steinvorth S, Corkin S, Halgren E. Ecphory of autobiographical memories: An fMRI study of recent and remote memory retrieval. Neuroimage 2006;30:285–298. [PubMed: 16257547]

Strang, G. Linear Algebra and its Applications. San Diego: Harcourt, Brace, Jovanovich; 1988.

Swanson LW, Wyss JM, Cowan WM. An autoradiographic study of the organization of intrahippocampal association pathways in the rat. J Comp Neurol 1978;181:681–716. [PubMed: 690280]

Taube JS, Burton HL. Head direction cell activity monitored in a novel environment and during a cue conflict situation. J Neurophysiol 1995;74:1953–1971. [PubMed: 8592189]

Taube JS, Bassett JP. Persistent neural activity in head direction cells. Cereb Cortex 2003;13:1162–1172. [PubMed: 14576208]

Taube JS, Muller RU, Ranck JB Jr. Head-direction cells recorded from the postsubiculum in freely moving rats. II. Effects of environmental manipulations. J Neurosci 1990a;10:436–447. [PubMed: 2303852]

Taube JS, Muller RU, Ranck JB Jr. Head-direction cells recorded from the postsubiculum in freely moving rats. I. Description and quantitative analysis. J Neurosci 1990b;10:420–435. [PubMed: 2303851]

Taube JS, Kesslak JP, Cotman CW. Lesions of the rat postsubiculum impair performance on spatial tasks. Behav Neural Biol 1992;57:131–143. [PubMed: 1586352]

Taube JS, Goodridge JP, Golob EJ, Dudchenko PA, Stackman RW. Processing the head direction cell signal: a review and commentary. Brain Res Bull 1996;40:477–484. [PubMed: 8886377]

Tsodyks MV, Skaggs WE, Sejnowski TJ, McNaughton BL. Population dynamics and theta rhythm phase precession of hippocampal place cell firing: a spiking neuron model. Hippocampus 1996;6:271–280. [PubMed: 8841826]

van Groen T, Wyss JM. The postsubicular cortex in the rat: characterization of the fourth region of the subicular cortex and its connections. Brain Res 1990;529:165–177. [PubMed: 1704281]

Wallenstein GV, Hasselmo ME. GABAergic modulation of hippocampal population activity: sequence learning, place field development, and the phase precession effect. J Neurophysiol 1997;78:393–408. [PubMed: 9242288]

Yoshida M, Hasselmo ME. Persistent spiking activity in neurons of the postsubiculum (dorsal presubiculum). Soc Neurosci Abstr. 2008in press

Yu X, Yoganarasimha D, Knierim JJ. Backward Shift of Head Direction Tuning Curves of the Anterior Thalamus: Comparison with CA1 Place Fields. Neuron 2006;52:717–729. [PubMed: 17114054]

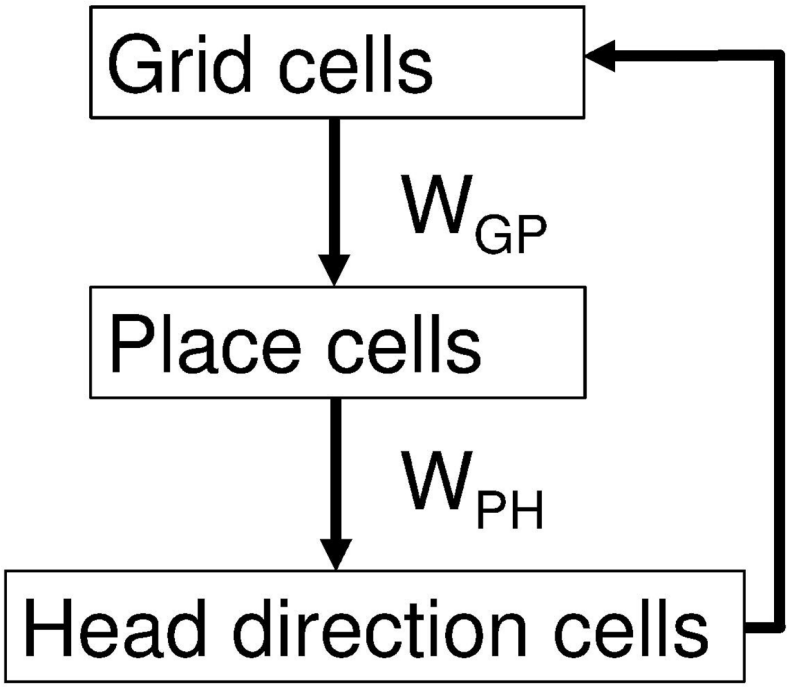

Figure 1.
Proposed episodic memory circuit for encoding and REM replay of trajectories using grid cells, place cells and head direction cells. Grid cells in medial entorhinal cortex (EC) are generated by speed modulated head direction input. The grid cells drive place cell firing in the hippocampus via synapses W_{GP}. During waking (encoding), links between state (place) and action (speed modulated head direction) are made by strengthening synapses between place cells and head direction cells W_{PH}. During retrieval, activity of place cells activates the associated head direction cells representing velocity. The head direction cells then update grid cells to activate place cells representing the next encoded location.

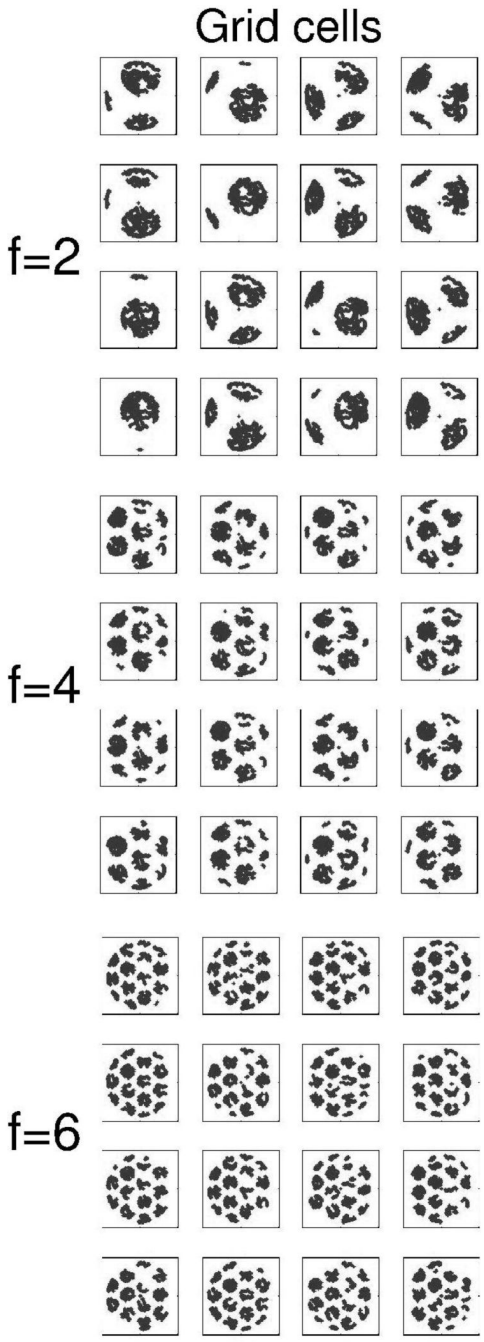

Figure 2.

Example of grid cell firing in the simulation. The model used a population of 75 grid cells during running on a circle task. The spatial periodicity of grid cell firing is illustrated in a smaller population of 48 grid cells during random foraging in an open field environment. Each square shows the pattern of firing of one simulated grid cell during the same open field trajectory. Firing fields are made up of many gray dots indicating the location of the virtual rat when the grid cell fires. Grid cells differ by baseline frequency in top (f=2), middle (f=4) and bottom (f=6) groups. Within each group, grid cells differ by initial phase of oscillation, with phase $\varphi=0$, $\pi/2$, π and $3\pi/2$. These simulations use the same orientation of $\phi=0$.

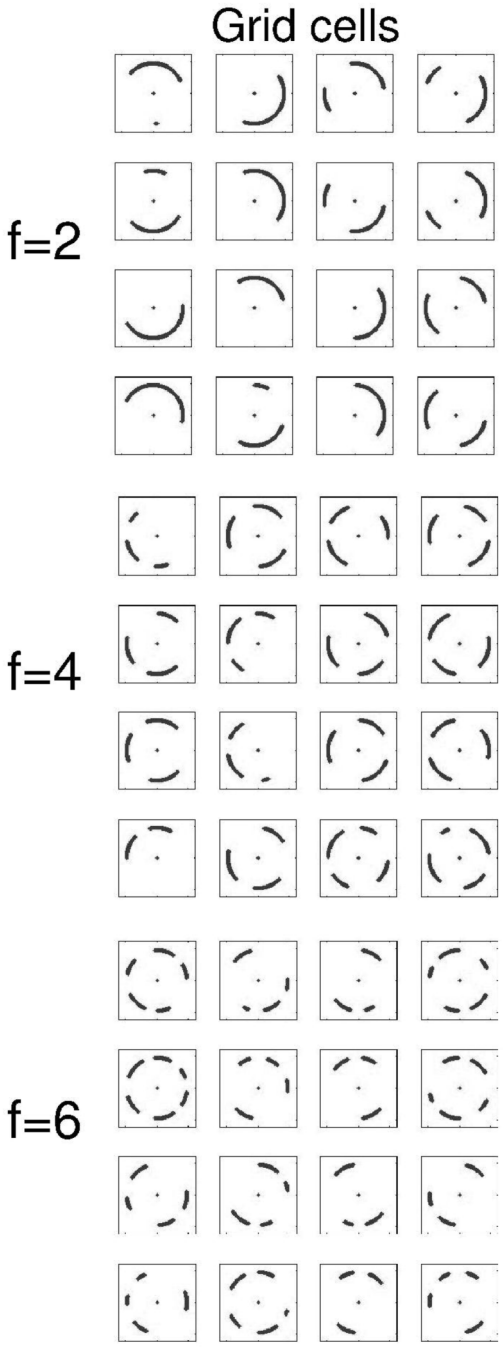

Figure 3.
Example of activity in the population of grid cells during running on the circular track. Each square shows the pattern of firing of one simulated grid cell during running on the circular track. Firing fields are made up of gray dots indicating location when grid cell fires. Grid cells differ by baseline frequency f=2,4,6 in groups. Within groups, grid cells differ by initial phase, with phase $\varphi=0, \pi/2, \pi$ and $3\pi/2$. As in Fig. 2, orientation $\phi=0$

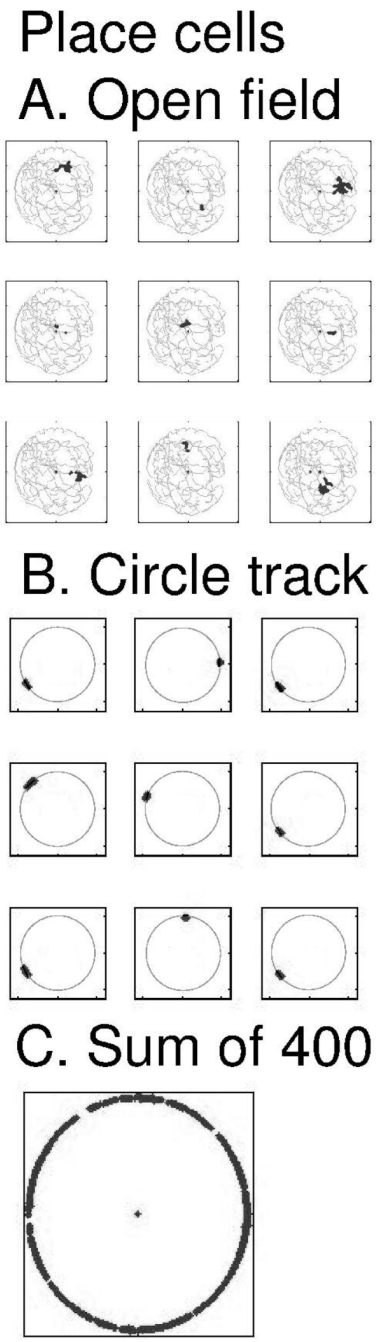

Figure 4.
Example of place cell firing in the simulation. The full simulation used 400 place cells. A. Examples of spiking activity of 9 place cells in an open field during a complex foraging trajectory (shown in gray). Black dots indicate location of rat when place cell fires. B. Example of 9 place cells during running on the circular track. Dots indicating location of the virtual rat when individual cells fired. Place cells fired in localized regions of the circular track. C. Simultaneous plot of the spiking activity of all 400 cells, showing that spikes occurred in individual place cells for almost all locations on the circular track.

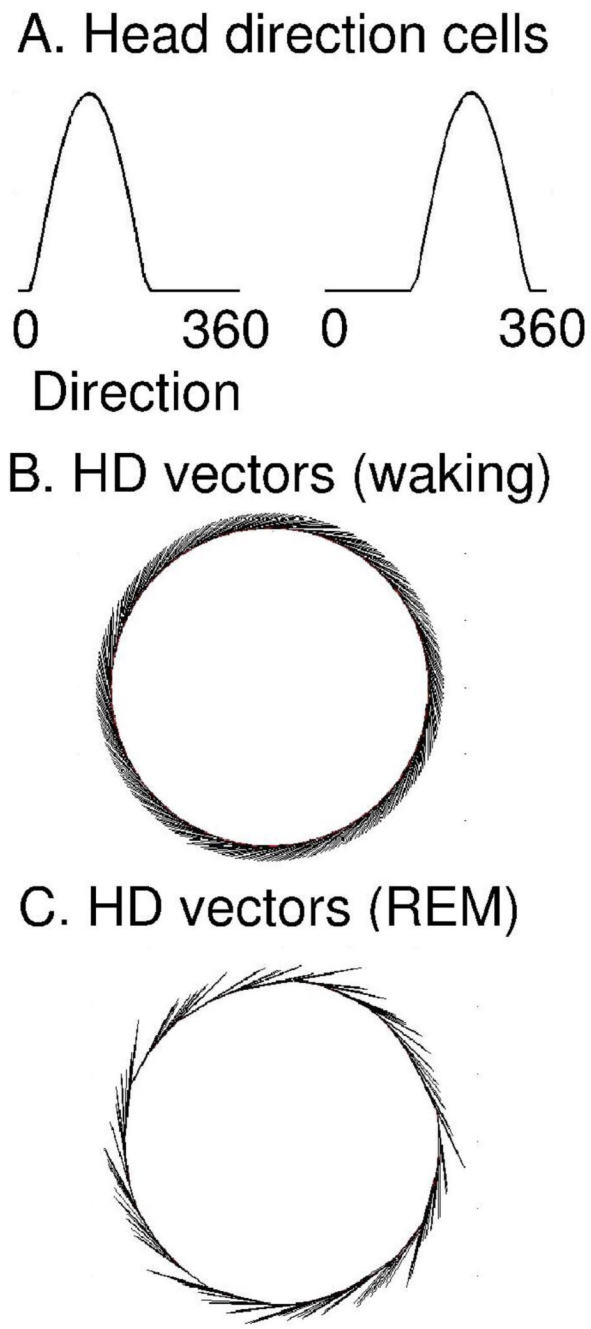

Figure 5.

A. Example of tuning of two head direction cells from the simulation, with preference for angles of 120 degrees and 240 degrees. B-C. Movement directions coded by the population of head direction cells during running on the circular track (95 cm diameter). Straight lines show the velocity vectors coded by head direction at each location. B. During waking (encoding), head direction cells driven by actual movement effectively code direction at each point in time, resulting in similar length and gradual shift in orientation of lines (for clarity, lines are shown for every 5th time step). C. During REM replay (retrieval), head direction cells are activated by the spread of activity from place cells. This results in retrieved velocity vectors that vary

somewhat in length and orientation, but effectively retrieve the circular trajectory (lines are shown for every time step).

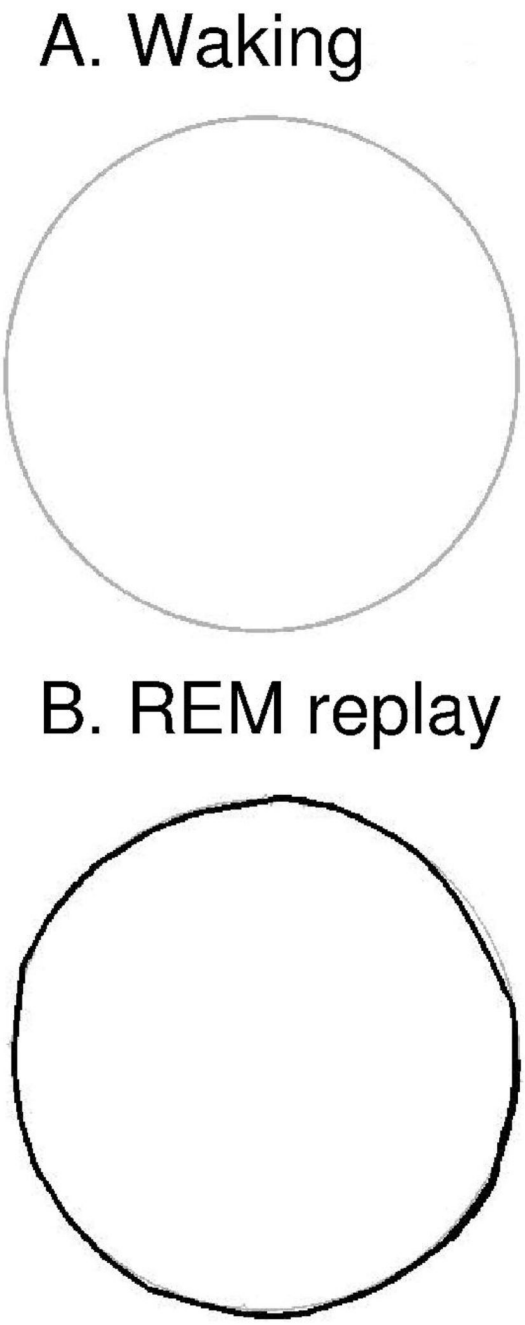

Figure 6.
The internal retrieval of trajectory during REM sleep matches the trajectory experienced during waking. A. The circular trajectory experienced and encoded during waking behaviour (95 cm diameter). B. The inverse transform of the phase of entorhinal grid cell oscillations during REM sleep shows that internal retrieval effectively replicates the original trajectory. The retrieval (black) covers the plot of the waking trajectory (gray).

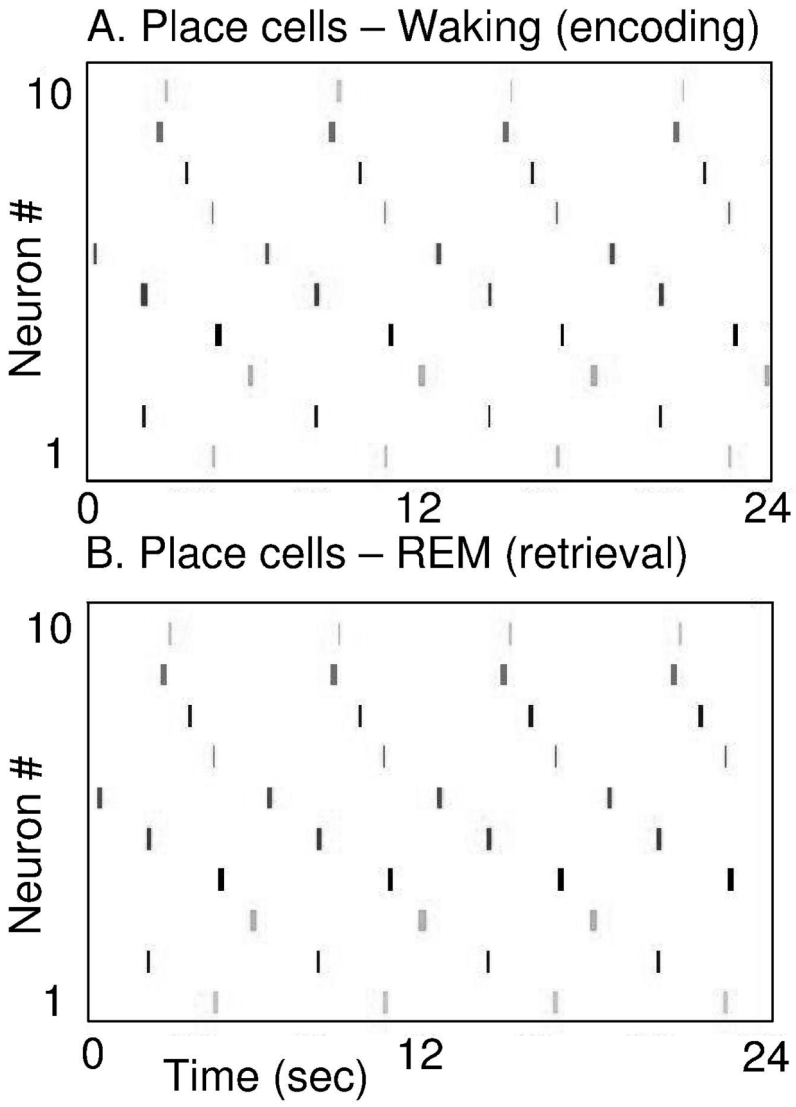

Figure 7.
Place cell activity during simulation of REM retrieval replicates the place cell activity during waking behavior. A. Spiking activity of 10 place cells during waking behavior. Spiking is shown in different rows during a period of 24 seconds of running the circular track, resulting in 4 full cycles of the track and 4 sequences of repeated spiking in the same place cells. B. Spiking activity of the same 10 place cells during simulated REM sleep (retrieval). Spiking is shown during a period of 24 seconds of simulated REM, during which the retrieval results in 4 full cycles of activation of the same sequence of place cells seen during waking.

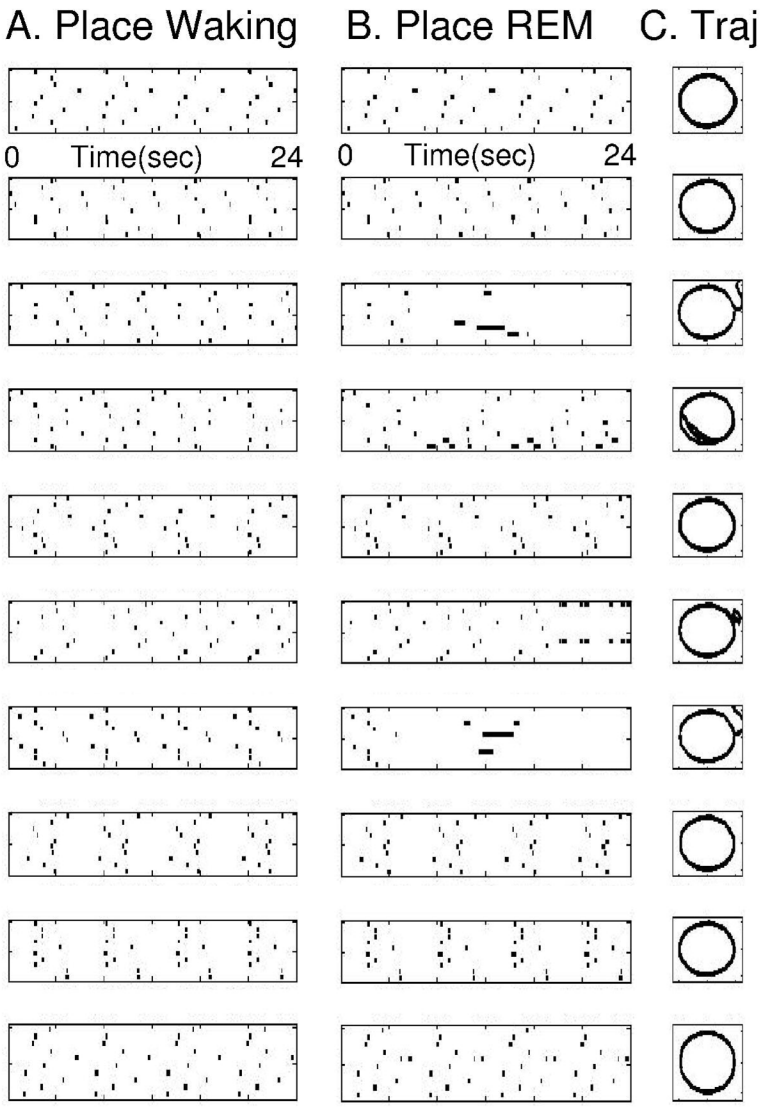

Figure 8.

Examples of place cell activity and retrieved trajectory during ten different simulations of the full model. Each row shows a separate simulation. Six out of ten simulations showed full replay during REM. Column A plots show spiking activity of 10 place cells during waking. Column B plots in the same row show spiking activity of the same 10 place cells during REM replay. Note similarity of patterns in Column B to Column A. Column C plots the inverse transform of grid cell activity during REM, showing successful retrieval of the circle in 6 out of 10 cases (track diameter 95 cm). In unsuccessful cases, the trajectory diverges from the circular track.

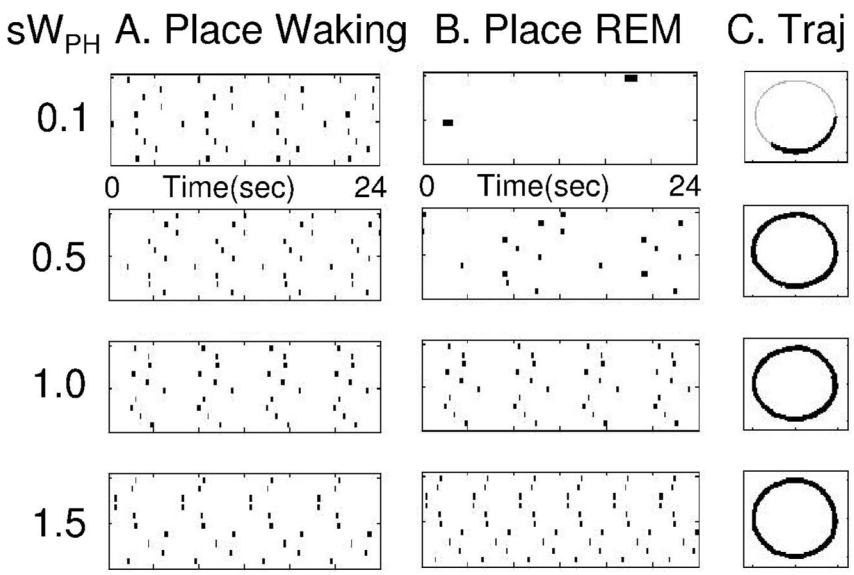

Figure 9.

Time course of REM replay determined by strength of connections from place cells to head direction cells W_{PH}. Column A shows place cell activity during waking, with same speed of movement. In each row of Column B, the connections W_{PH} are multiplied by a different value during REM replay. This results in different speeds of replay relative to waking, with s=0.1 resulting in less than 1/2 cycle, s=0.5 resulting in 2 cycles during 24 seconds, s=1.0 resulting in 4 cycles, and s=1.5 resulting in 6 cycles during 24 seconds.

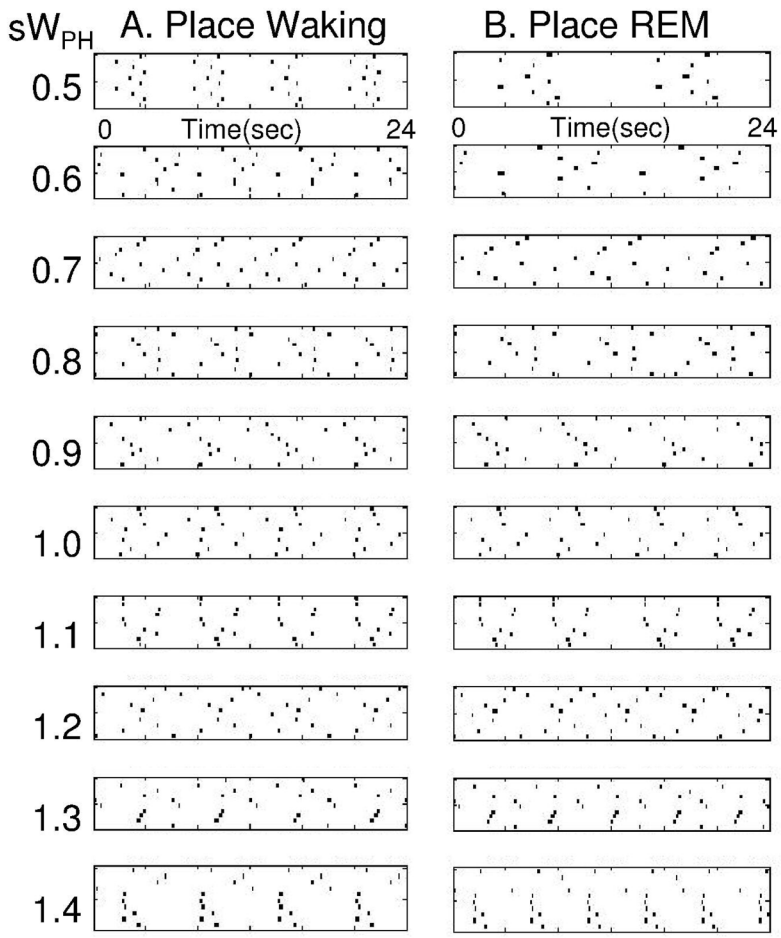

Figure 10.

Ten examples of REM replay with different strengths of connections from place cells to head direction cells W_{PH}. Column A shows place cell activity during waking, with same speed of movement. In each row of Column B, the connections W_{PH} are multiplied by a different value during REM replay. This results in different speeds of replay relative to waking.

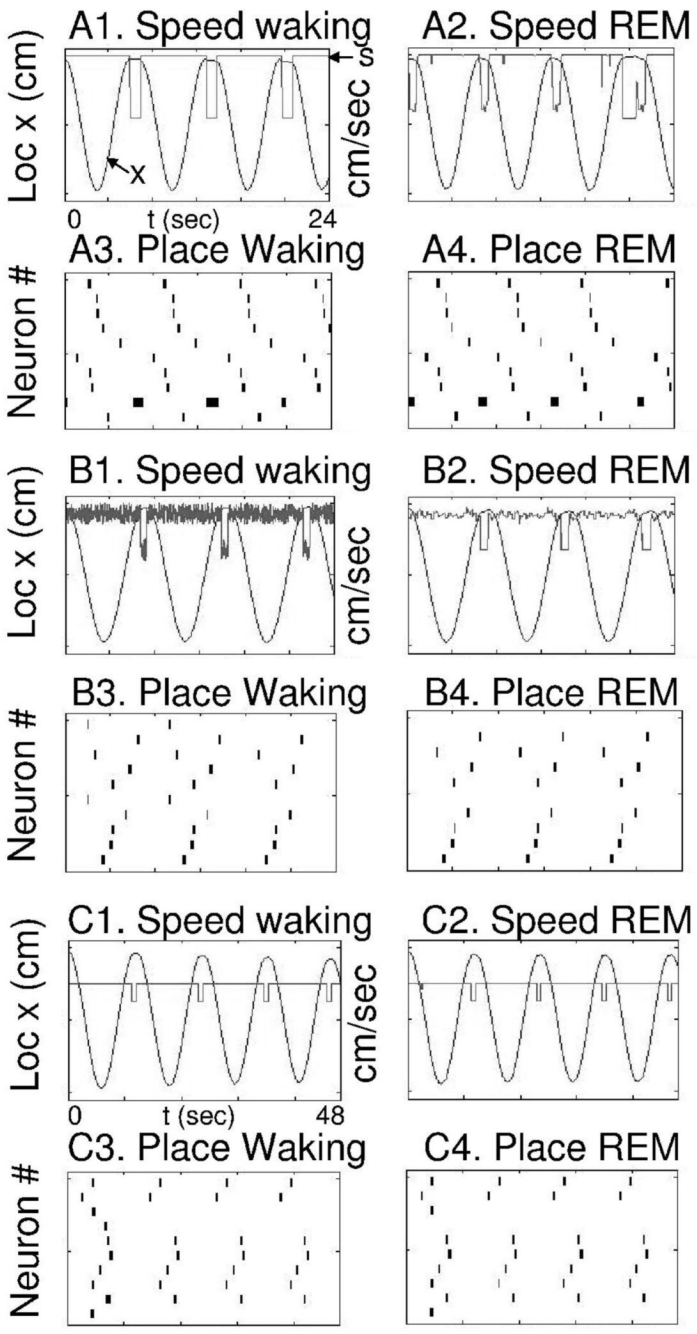

Figure 11.

REM replay can replicate changes in running speed during waking. A1. During waking, location (in cm) changes cyclically as rat traverses circular track (line marked x). Top line on same plot shows speed in cm/sec (line marked s), starting with a steady speed of 50 cm/sec, and reducing to 5 cm/sec during each approach to the reward location (when x approaches 50 cm). A2. REM replay shows the same slowing of speed near the reward location. A3. Place cell firing during waking shows extended place cell activity near reward location that also occurs during REM replay (A4). B1. Network performance is similar with addition of noise to the movement speed during waking. To show the capacity to replicate different speed changes, the external change in speed goes from 50 cm/sec to 25 cm/sec near reward location. B2. REM

replay shows similar changes in speed (note similar pattern of noise on each cycle). B3. Place cell activity during waking resembles place cell activity during REM replay (B4). C1. The network performance is similar when movement starts at 25 cm/sec and reduces to 12.5 cm/sec near reward. C2. REM replay shows similar changes in speed, and place cell activity during waking (C3) resembles that during REM replay (C4). Note that plots show 24 sec in A and B and 48 sec in C.

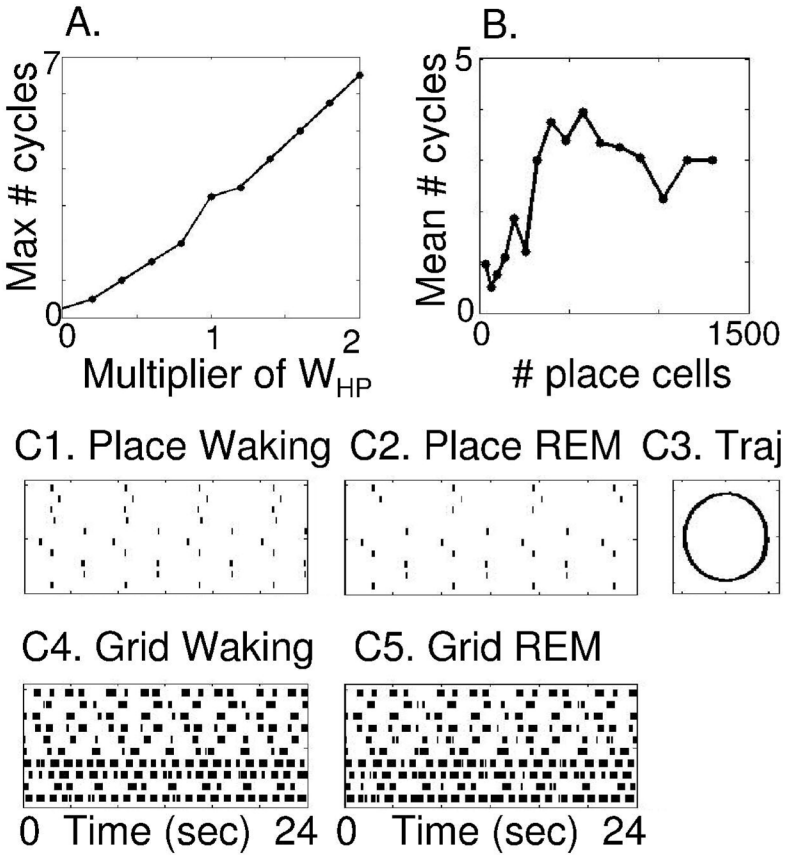

Figure 12.

Number of cycles of successful REM replay with changes in different parameters. A. The number of cycles of REM replay increases in proportion to the multiplier of W_{PH}. B. The number of cycles of successful REM replay depends upon total number of place cells, with good performance starting at 324 cells and remaining high for larger numbers. C. This model simulating place cell activity during waking (C1) and REM sleep (C2) generates the prediction that grid cell activity during REM sleep (C5) should correlate with grid cell activity associated with running the circular track during waking (C4).